A mechanistic basis for understanding the dual activities of the bifunctional *Azotobacter vinelandii* mannuronan C-5 epimerase and alginate lyase AlgE7

Margrethe Gaardløs[1], Tonje Marita Bjerkan Heggeset[1,2], Anne Tøndervik[2], David Teze[3,4], Birte Svensson[3], Helga Ertesvåg[1], Håvard Sletta[2] and Finn Lillelund Aachmann[1]*.

[1]Norwegian Biopolymer Laboratory (NOBIPOL), Department of Biotechnology and Food Science, NTNU Norwegian University of Science and Technology, Sem Sælands vei 6/8, N-7491 Trondheim, Norway

[2]Department of Biotechnology and Nanomedicine, SINTEF Industry, Postboks 4760 Torgarden, N-7465 Trondheim, Norway.

[3]Department of Biotechnology and Biomedicine, Technical University of Denmark, DK-2800 Kgs. Lyngby, Denmark.

[4]Novo Nordisk Foundation Center for Biosustainability, Technical University of Denmark, DK-2800 Kgs. Lyngby, Denmark.

***Corresponding Author:** Finn Lillelund Aachmann, finn.l.aachmann@ntnu.no , +47 97 95 48 59.

Keywords: Alginate, alginate C-5 epimerase, alginate lyase, multifunctional enzyme, site-directed mutagenesis. nuclear magnetic resonance (NMR), time-resolved NMR, enzyme mechanism.

Running title: Bifunctional Alginate Epimerases and Lyases

Abstract

Mannuronan C-5 epimerases and alginate lyases are important enzymes for tailoring of the functional properties of alginate. The reaction mechanisms for the epimerization and lyase reactions are similar, and some enzymes, like AlgE7 from *Azotobacter vinelandii,* can perform both reactions. These enzymes share high sequence identity with mannuronan C-5 epimerases without lyase activity, and the mechanism behind their dual activity is not understood. In this study, we investigate mechanistic determinants involved in the bifunctional alginate lyase and epimerase activity of AlgE7. Based on sequence analyses a range of AlgE7 variants were constructed and subjected to activity assays and product characterization by NMR. Calcium promotes lyase activity whereas NaCl reduces the lyase activity of AlgE7. By using well-defined alginate substrates, the preferential cleavage sites of AlgE7 are found to be M|XM and G|XM. From the study of variants, it was found that R148 is particularly important for the lyase activity of AlgE7, and we obtained pure epimerase variants. Furthermore, the results suggest a catalytic reaction mechanism, with H154 as the catalytic base and Y149 as the catalytic acid. This study opens for further applications of alginate epimerases and lyases, by providing a better understanding of the reaction mechanism and how the two enzyme reactions can be altered by changes in reaction conditions.

Introduction

Alginate-modifying enzymes, and in particular epimerases and lyases, can be used to tailor the physical properties of alginate products for food, medicine and material purposes (1–4). Epimerization of β-D-mannuronic acid residues (M) into α-L-guluronic acid residues (G) by mannuronan C-5 epimerases creates non-random block patterns of epimerized residues, forming stretches of consecutive G-residues (G-blocks), M-residues (M-blocks), and alternating MG-residues (MG-blocks) in the alginate (5, 6). M-residues are found in a $^{4}C_{1}$ chair conformation, whereas G-residues take on a $^{1}C_{4}$ conformation, giving rise to distinct structures of the blocks. The M/G composition of the alginate together with the molecular weight determine the properties and application areas of the polymers including gel-forming abilities (7). Gel-formation of alginate happens when G-blocks, and to some extent MG-blocks, cross-link with other chains through junction zones coordinated by divalent cations like calcium (8). Alginate lyases catalyse the depolymerisation of alginate by a β-elimination mechanism, generating an unsaturated 4-deoxy-L-*erythro*-hex-4-enepyranosyluronate residue (denoted Δ) at the non-reducing end and a new reducing end (9). The enzymatic post-polymerization modifications by epimerases and lyases are therefore important for functional properties of the polymers related to its viscosity and gel-forming abilities. Two main types of bacterial epimerases are characterized at present: the periplasmic, calcium-independent AlgG, found in species of *Pseudomonas* and *Azotobacter*, and the extracellular, calcium dependent AlgE, found in *Azotobacter* sp. and some strains of *Pseudomonas*. The AlgE epimerases comprise seven well-studied enzymes from *A. vinelandii* (AlgE1-7) (10, 11), PsmE from *P. syringae* (12), and three recently identified *A. chroococcum* enzymes (AcAlgE1-3) (13). Fourteen polysaccharide lyase (PL) families in the Carbohydrate-Active enZYmes (CAZy) database have so far been described to include alginate lyases, where they are characterized based on their overall structure, catalytic amino acids residues, and mode of action (14, 15). Alginate lyases can have either mannuronate (EC 4.2.2.3) or guluronate lyase activity (EC 4.2.2.11), and some are reported to have both activities.

The distinct patterns of MG-blocks and G-blocks created by the AlgE epimerases can be caused either by preferred attack or from a processive mode of action. Studies have shown evidence for the processive mode for AlgE4, and it is hypothesised that the enzyme epimerizes every other sugar residue processively upon each binding event (16, 17). Such an action would create MG-blocks from the first binding event and G-blocks from the second, explaining the occurrence of both block structures. Enzyme residues involved in substrate recognition are important for substrate specificity in a preferred attack of epimerized sequences as well as for a processive movement along the substrate. Previous studies show that minor sequence differences affect activity and product pattern, through substrate interaction with residues far from the active site (18–22).

Epimerases and lyases acting on alginate are thought to share a similar reaction mechanism (Figure 1) (9). The first step, involving the catalytic base (denoted AA2 in Figure 1), is common for both reactions, whereas the difference lies in the step involving proton donation (by AA3 in Figure 1). Here, a proton donated to C5 from the opposite side of the sugar ring results in epimerization, whereas a proton donated to the glycosidic bond results in cleavage. AlgE7 and the two *A. chroococcum* epimerases AcAlgE2 and AcAlgE3 display both lyase and epimerase activities, highlighting the similarity in the mechanisms. It has been suggested that the dual activities originate from the same active site (23). All alginate epimerases share a common YG(F/I))DPH(D/E) motif, conserved as ^{149}YGFDPHE in the AlgEs (numbering according to AlgE7). The enzyme residue(s) contributing to cleavage are probably found outside of this motif, which is conserved also for the bifunctional AlgE enzymes. These determinant residue(s) could work either directly as a proton donor in the lyase reaction, or by affecting a common AA3 to perform

both cleavage and epimerization events. In the YGFDPHE motif, the tyrosine (Y149) and the histidine (H154) are thought to be the catalytic base and acid (represented as AA2 and AA3 in Figure 1). Notably, which of these residues actually acting as the catalytic base is still not known (19, 24). For *P. aeruginosa* AlgG, which has a similar active site to the AlgE enzymes despite low overall sequence similarities, it has even been proposed that water serves as the catalytic acid and that the tyrosine has a role in substrate recognition (24). The aspartate in the motif (D152) might have a role in positioning of the histidine (24). The glutamate in the motif (E155) could stabilize the substrate carboxylate group through coordination of a calcium ion, together with D178 that is conserved in the AlgE epimerases, but not in the calcium independent AlgG epimerases (19, 24). If this is the case, the calcium ion would represent AA1 in Figure 1. It is important to note that calcium is required for the structural stability of the active modules (A-modules) of the AlgE, as well as for the CBM-like R-modules that are present in from one to seven copies in the AlgEs (19, 25, 26). It has however not been confirmed whether the calcium dependency of the AlgE enzymes is also directly linked to a catalytic role. If they are not involved in calcium coordination, the three acidic residues in the active site could have roles in modulating the pK_a-values of the other residues in the active site, which are essential for the acid/base mechanism.

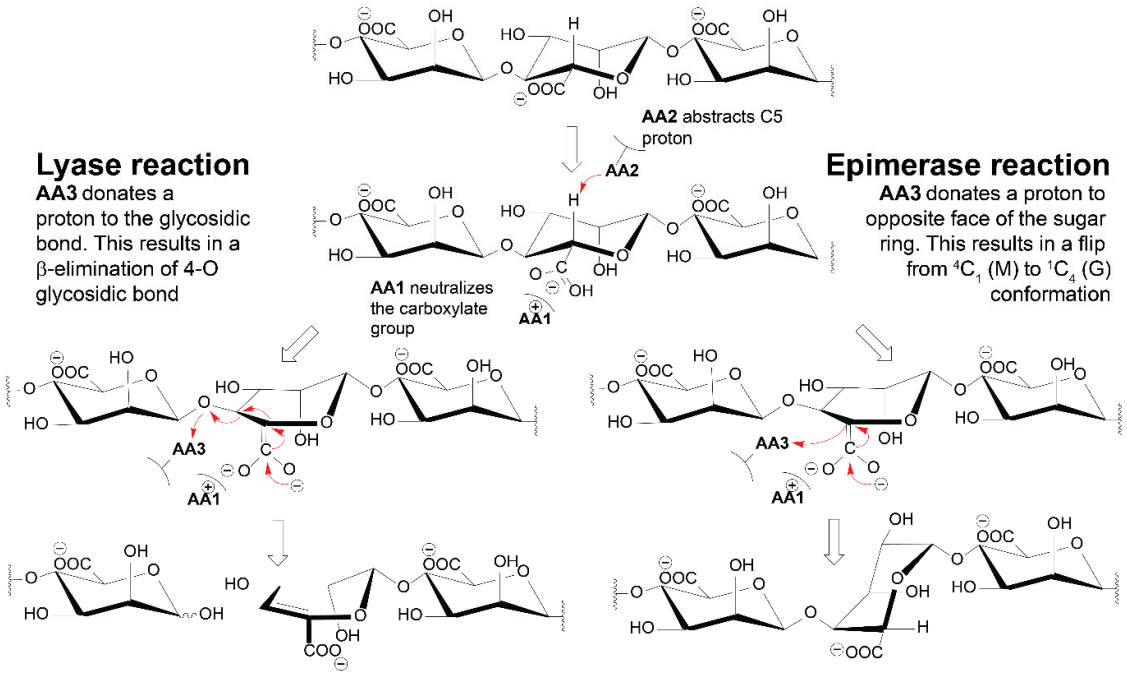

Figure 1: Proposed alginate lyase and epimerase reaction mechanisms. Both mechanisms start with proton abstraction from C-5 by AA2 (amino acid 2), requiring a charge neutralization of the carboxylate by AA1. In the lyase reaction, a proton is donated to the leaving group of the glycosidic bond, whereas in the epimerase reaction a proton is donated to the sugar ring to create the epimer. Only the M-lyase reaction is shown in the figure.

Here we investigate the mode of action of the dual activity of AlgE7 and elucidate the catalytic mechanism through creating enzyme variants with amino acid substitutions in and around the active site. The mode of action is further explored under different reaction conditions varying the concentrations of NaCl, substrate, and $CaCl_2$, as well as pH.

Results

Elucidation of the catalytic lyase/epimerase mechanism

The lyase and epimerization activities are mutually dependent

The epimerization pattern and preferred cleavage sites of AlgE7 have been studied previously (11, 23), but the mode of action is not understood. To verify the end products and further elucidate the mode of action, we have used ^{1}H NMR at different reaction time points, time-resolved ^{13}C NMR, and ^{13}C HSQC (Heteronuclear single quantum coherence spectroscopy) spectra (Figure 2, Figure S1, and Table S1). The lyase and epimerase activities are closely linked in how they affect each other in the creation of the product pattern. The ^{1}H NMR spectrum of AlgE7 wild type displayed in Figure 2A on polymannuronan (polyM) alginate shows an absence of ΔG-signals and approximately equal amounts of M- and G-residues at reducing ends, corresponding to the potential cleavage sites G↓MM, G↓GM, M↓GM and M↓MM (where cleavage of the 4-O glycosidic bond happens at the arrow shown in the indicated sequences). As a distinction between Δ-residues coming from M or G cannot be made, the potential cleavage sites are denoted here as G↓XM and M↓XM. The decline in G-residues, seen as a decreasing F(GG) during the reaction course, implies that X could be a G-residue and that AlgE7 is able to abstract a proton from G-residues. From the time-resolved ^{13}C NMR-spectra (Figure 2B), we can infer that AlgE7 likely is able to abstract H-5 from M-residues, as <u>Δ</u>M is created from the start. The <u>Δ</u>M-peak is much larger than the Δ<u>M</u>G-peak, suggesting that there is more ΔMM created, and this is supported by the HSQC-spectrum recorded at the end of the reaction (Figure S1). Since we see <u>G</u>G-signals in the proton spectrum after 60 h, GGM triads could have been turned into GG-red and Δ. No G-block signals were present in the HSQC-spectra from AlgE7 on polyM.

The results suggest that AlgE7 has a preference for cleaving G↓XM, in agreement with Svanem et al. (23). However, if the enzyme indeed has this preference, it would be expected that more G-reducing ends are formed during the reaction course when the G-content increases as a result of epimerization. From the integrals of the ^{1}H-spectra in Figure 2A, however, the formation rates of both M- and G-reducing ends were about the same for the duration of the reaction. When polyMG was used as substrate, the pattern changed. The ^{1}H- and time-resolved spectra show that the lyase activity decreased, a small ΔG signal appeared, and almost no M_{red} was created. This finding corresponds to a weak activity on the cleavage site G↓XG, which was not found on polyM. From the time-resolved spectra we see that a G-block rich alginate is produced, as the MG-blocks are filled in. A total lack of activity was found on pure oligo-G, excluding cleavage inside G-blocks (Figure S2). In conclusion, the degree to which the substrate is epimerized appears to be highly important for the lyase activity.

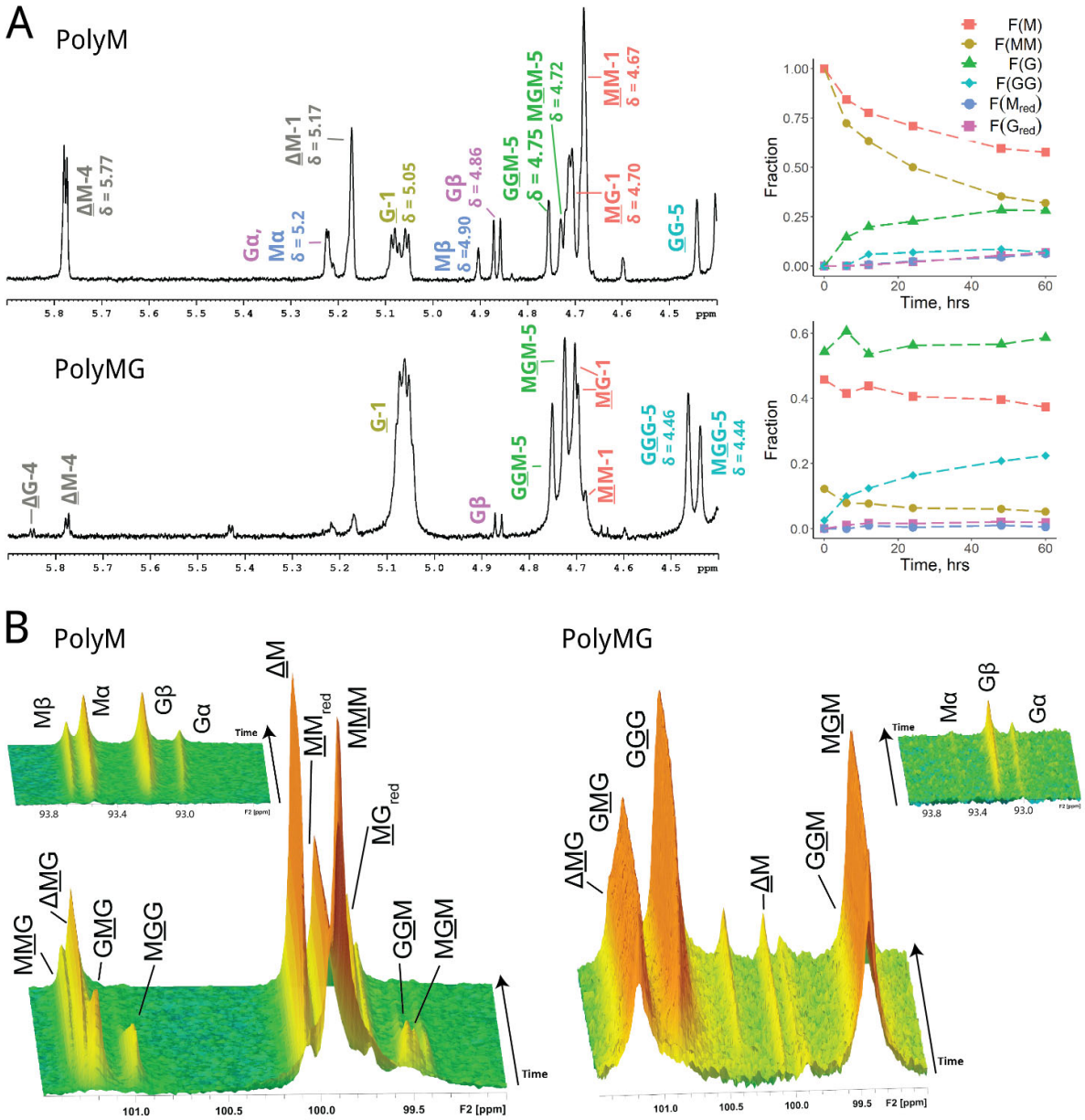

Figure 2: NMR spectra showing AlgE7 acting on polyM and polyMG. Underlined monomer residues give rise to the signals, and they give distinct peaks based on their nearest neighbour residues. A: ^{1}H spectra after epimerization for 60 h. 5 mM HEPES, 75 mM NaCl, 2.5 mM $CaCl_2$, pH 7.0. 2.5 mg/ml of substrate and 92 nM of enzyme were used in the reaction (1:300 enzyme:substrate (w/w)). Fractions of residues calculated from integration of the ^{1}H-spectra at different time points are plotted to the right and shown in Table S1 (calculation of sequential parameters explained in Figure S3). B: Time resolved ^{13}C-spectra of the reaction from 0-1000 min (16.7 h), recorded at 25 °C with 10 mM MOPS, 75 mM NaCl, 2.5 mM $CaCl_2$ and pH 6.9. 11 mg/ml of substrate and 2.9 µM of enzyme were used (1:42 enzyme:substrate, w/w).

The spectra shown in Figure 2A and B were recorded with 75 mM NaCl, but ^{1}H NMR-spectra were also recorded without NaCl in the buffer. The product pattern changed somewhat, especially on polyMG where NaCl enhances epimerization (Figure S4 and Table S1). ^{13}C NMR-experiments on polyM without NaCl showed the same trends as discussed here, except for a total lack of MGG-signals during the reaction course. Lyase activity seems to be more dominating in the absence of salt, and this was investigated in more detail (see later section).

High-Performance Anion-Exchange Chromatography with Pulsed Amperometric Detection (HPAEC-PAD) was run for the samples epimerized for 60 h in presence of NaCl (Figure S5). AlgE7 displays a pattern that is different from the M-and G-specific lyases acting on similar substrates, reflecting the more complex product patterns caused by cleavage of epimerized samples. The products created by AlgE7 overlap approximately with the trimers through hexamers created by an M-specific lyase on polyM and polyMG, whereas the peaks do not overlap with the pure G-oligomers created by the G-specific lyase on polyG.

Molecular basis for the lyase activity of the bifunctional enzymes and identification of R148 as a central residue

To understand the dualistic activity of AlgE7, we wanted to see if the ratio between the two activities could be affected by creating amino acid substitution variants of the enzyme. It has been proposed that there is one active site, containing the four catalytic residues Y149, H154, D152, and D178, responsible for both the lyase and the epimerization reaction (23). With this assumption, we examined sequence differences in the substrate binding groove and around the active site. Svanem et al. (2001) showed that exchanging the N-terminal 266 amino acids in AlgE1 with the corresponding sequence of AlgE7 (creating the chimeric enzyme AlgE7-AlgE1) resulted in a bifunctional enzyme. The mutational study was therefore focused on the N-terminal part (residue G100-I200) of AlgE7, i.e. the A-module.

Several amino acid residues in the binding groove differ between the bifunctional lyases/epimerases and the epimerases. This is illustrated in an alignment of the protein sequence of AlgE7A, compared to the consensus sequences of the three bifunctional A-modules (ConL) and the ten epimerase A-modules from *A. vinelandii* and *A. chroococcum* (ConE) (Figure 3A, Figure S6). An extensive hydrogen bonding network is formed in the binding groove, illustrated with dashes in Figure 3B. Such networks have earlier been shown to be important for the binding and processive action of epimerases (21). AlgE7 and the other bifunctional AlgE contain some

charged and polar residues not present in the AlgE epimerases (specifically Y122, R148 and K172) (Figure 3).

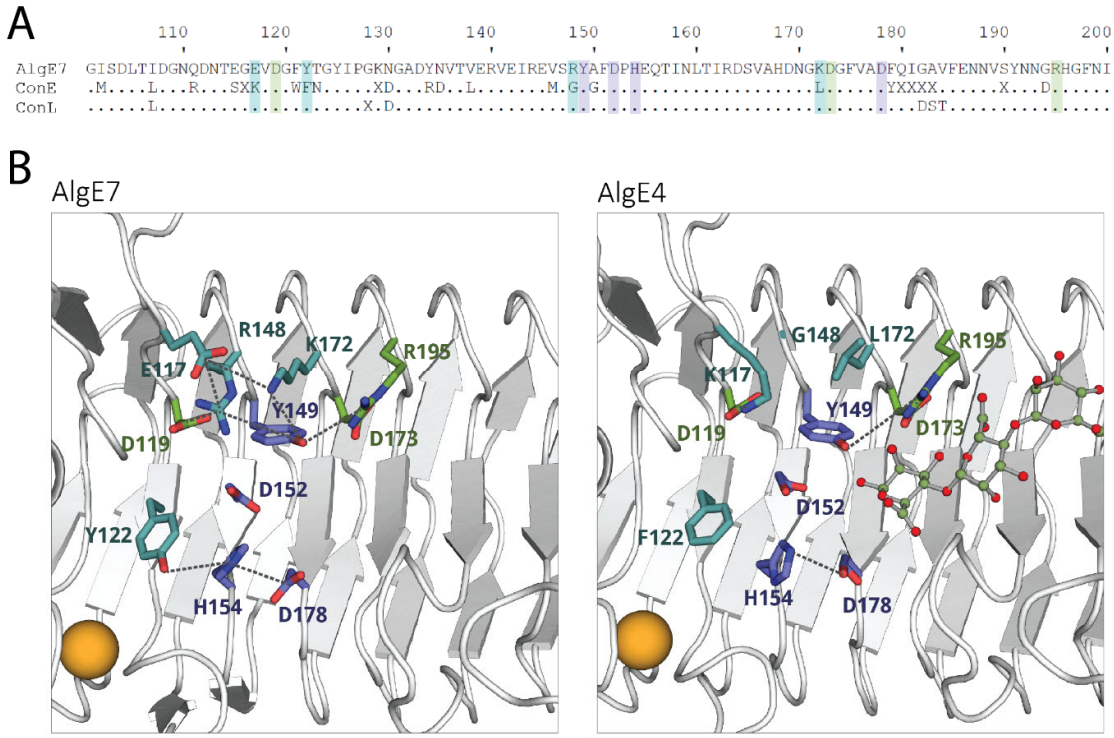

Figure 3: A: Alignment of AlgE7 from *A. vinelandii* with two consensus sequences. ConE is the consensus sequence of the A-modules displaying only epimerase activity from *A. vinelandii* and *A. chroococcum* (AlgE1A1, AlgE1A2, AlgE2A, AlgE3A1, AlgE3A2, AlgE4, AlgE5, AlgE6, and AcAlgE1. ConL is the consensus of the A-modules that have both lyase and epimerase activity (AlgE7, AcAlgE2A, and AcAlgE3A). Residues that are not conserved in the consensus sequence are represented in the alignment as "X", whereas dots denote residues that are almost or completely conserved. Highlighted letters indicate amino acids replaced in this study: Purple are the catalytic amino acids, blue are the four residues differing between ConE and ConL, and green are other studied residues. AlgE7 has 82 % identity with ConL and 63 % identity with ConE. The alignment and consensus sequences are made from global protein alignments using BLOSUM 62 scoring matrix. B: The residues highlighted in A, shown in sticks in the crystal structure of AlgE4 (right) (2PYH) and a homology model of AlgE7 (left), with the same colour code as the highlights in A. Dashes are shown between residues that potentially form hydrogen bonds. The calcium ion needed for structural stability is visualised as an orange sphere. The model was built by SWISS-MODEL (27), using the structure of AlgE4 (2PYH.pdb), then energy minimized through the YASARA server *(28)*.

Thirty-tree single amino acid replacements and combination variants of AlgE7 were created in total, based on sequential and visual analysis as illustrated in Figure 3. The following paragraphs will describe each group of the created variants in more detail. Results from two activity assays are shown in Table 1. In the ^{3}H-assay, the release of ^{3}H from [5-^{3}H]-labelled mannuronan is detected (29, 30). This assay is thus a direct measure for the first step of the reaction (Figure 1), where a proton is abstracted from the substrate. Since this step is common for both activities, the ^{3}H-assay measures the total enzyme activities. In the lyase assay, activity is measured by detecting the increase in absorbance at 230 nm upon generation of the unsaturated double bonds in the resulting Δ-residues (Figure 1). We measured the absorbance with five minutes intervals for the reaction duration, and the initial slope was calculated and compared to that of the wild type. For twenty-two of the variants we also performed an enzymatic reaction for 48 h, and analysed the product profiles at the end of the reaction with ^{1}H NMR. Results from eighteen of these variants are shown in Figure 4, whereas D119A, D119N, Y122A and D173A had no detectable activity and are excluded from the figure (values are listed in Table S2). These experiments were performed using partially purified enzyme extracts where

the exact enzyme concentrations cannot be determined. Therefore, the results in Table 1 and Figure 4 describe qualitative differences between the variants.

Table 1: Results from ^{3}H assay and lyase assay of AlgE7 variants on polyM. All results are in percentage of wild type (wt). Bright green indicates activity between 60-100 % of wild type, dark green is activity above 100 % of wild type, light green is between 20-59 % of wild type and pale green is between 1-19 % of wild type. An asterisk (*) denotes residues involved in catalysis. ND (not determined) denotes that the experiment has not been performed. In the ^{3}H assay, 0.25 mg/ml of [5-^{3}H]-poly M was incubated with 2 mM $CaCl_2$ and enough enzyme extract (from 5-100 µL in 0.6 ml total volume) to give comparable signals. In the lyase assay, 20 µL of enzyme extracts were added to a total of 250 µL reaction buffer containing 2.5 mM $CaCl_2$ and 1 mg/ml polyMl.

Mutation	^{3}H [%]	Lyase [%]
wt	100	100
E117K	>100	77
E117L	ND	92
D119A	2	0
D119E	9.4	3.1
D119N	0.5	0
Y122A	ND	0
Y122F	2.5	3.3
Y149A *	0.6	0
Y149F *	0.6	0
Y149H *	0.5	ND
R148G	1.9	1.9
R148K	2.2	7.7
D152E *	0.2	0
D152N *	2.0	0
H154F *	0.1	0
H154Y *	0.3	0
K172L	76	77
K172R	>100	>100
D173A	ND	0.7
D178E *	0.1	0
D178N *	0.8	0
D178R *	0.3	0
R195L	3.7	0

Mutation	^{3}H	Lyase
E117K + R148G	ND	4.0
E117K + R148G + K172L	ND	3.8
R148G + K172L	1.8	0
R148G + K172R	1.1	0
E117K + Y122F + R148G	1.3	0
E117K + Y122F + K172L	4.3	40
E117K + Y122F + K172R	3.6	32
E117K + Y122F + R148G + K172L	3.6	0
E117K + Y122F + R148G + K172R	5.6	0
E117K + Y122F + Y149A	1.2	0

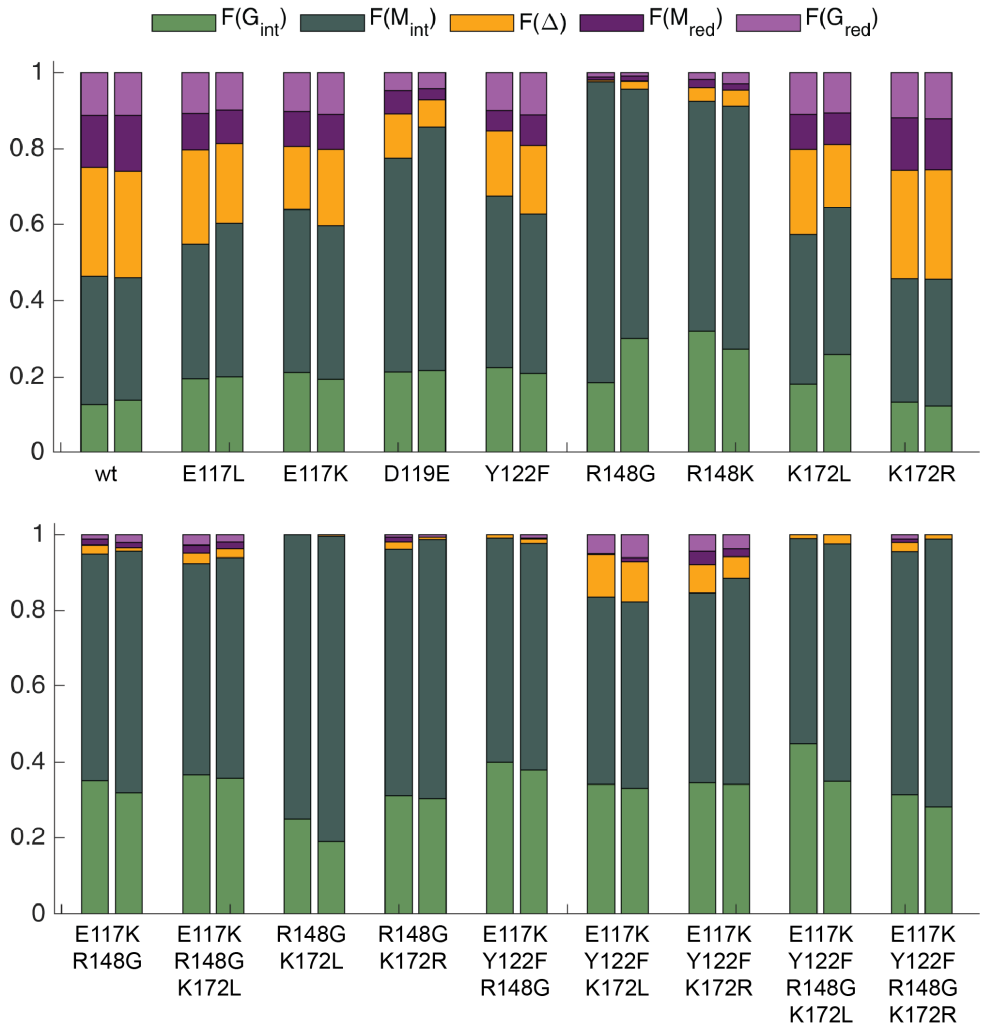

Figure 4: Product profiles from end point ^{1}H NMR of wild type and variants acting on 1 mg/ml polyM, with 2.5 mM $CaCl_2$ added to the reactions, incubated at 25 °C for 24 hours. 40 µL of enzyme extracts were added to 500 µL reaction. Each column represents one experiment, and duplicates are positioned together. Green, internal G-residues; orange, Δ-residues; dark green, internal M-residues; dark purple, M-residues at reducing ends; and light purple, G-residues at reducing ends. The sum of these fractions amounts to 1.

Residues E117, Y122, R148, and K172 are all invariantly conserved in the bifunctional enzymes, whereas K117, F122, G148, and L172 are conserved in the epimerases. In the epimerases, K117 forms a salt bridge with the conserved residue D119. In the bifunctional enzymes residue 117 is a glutamate, and the positive charge interacting with D119 is instead provided by R148. K172 in the bifunctional enzymes introduces an additional positive charge close to the active site residue Y149. Y/F122 is the only of the four residues situated close to the catalytic histidine, and it introduces a polar group to the active site. By exchanging all four residues and combinations of them into the corresponding residues found in the epimerases (E117K, Y122F, R148G, and K172L), we wanted to see if the lyase activity could be suppressed, and in that case which of these residues exerted the largest effect on the activity. The variants E117L, Y122A, R148K, and K172R were created to investigate the role of the side chains further, and K172R was also included in the combination variants.

The most interesting single variant turned out to be R148G, which almost completely abolished the lyase activity while preserving the epimerase activity (Table 1 and Figure 4). The

variant R148K retained a reduced yet significant lyase activity. Because of its significance for the lyase activity, we also purified the R148G variant and performed the same ^{1}H-NMR, time-resolved ^{13}C-NMR and HSQC experiments as for the wild type presented above, on both polyM and polyMG (Figure 5, Figures S1-S4, Table S1). From the plot of ^{1}H-NMR integrals on polyM, we see that R148G produces G-residues and GG-dyads like the wild type, but at a slower rate. On polyMG, it also displays the ability to create longer G-blocks, from the appearance of the GGG-peak, similar to the wild type. We also performed the same experiment without the addition of NaCl (Figure S4), and under these conditions the GGG-peak did not appear. As with the wild type, it is clear that NaCl affects the epimerisation activity, especially for the ability of the enzymes to create G-blocks on polyMG.

In contrast, E117K/L and K172L/R retain lyase activity (Table 1) and product profiles (Figure 4, Table S2) that are similar to the wild type. Y122F has reduced total activity and lyase activity as measured in the assays in Table 1, but displays similar product profiles at reaction completion, indicating that the activity differences observed could be due to a slower initial activity. By combining E117K, Y122F and K172L/R, the total activity and lyase activity are similar to that of R148G/K, whereas its product profile shows a higher lyase- and epimerase ability than R148G/K. This points to indirect roles of these three residues in catalysis, as their replacements are not detrimental to the lyase activity. Nevertheless, E117L/K, Y122F and K172L appear to be connected to substrate specificity, as they produce higher amounts of G_{red} than M_{red} as opposed to the wild type that produces slightly more M_{red}. The combination variant containing E117K, Y122F and K172L produces almost exclusively G_{red}. All other combination variants contain R148G, and they have low initial activities and very low levels of lyase end products. Unlike Y122F, Y122A was inactive.

The role of D119, which as mentioned is associated through salt bridges with K117 in the epimerases and R148 in the bifunctional enzymes, was investigated through the variants D119A, D119N and D119E. Of these, D119E retained almost 10 % of wild type total activity, and around 31 % of lyase activity, whereas D119A and D119N only retained from 0.5-2 % of wild type activity (Table 1). Of the three, only D119E had detectable activity in the ^{1}H-NMR experiment, but reduced lyase activity compared to the wild type (Figure 4). It also produced an alginate with more G-residues, but this could be a result of a lower lyase activity. D173 and R195 are positioned close to the catalytic Y149, and these three residues are part of a hydrogen bond network. We created D173A and R195L in order to elucidate their role. As seen in Table 1, the AlgE7 D173A variant displayed a measurable lyase activity, but too low to be detected in the ^{1}H-NMR experiments. R195L has no detectable lyase activity, but displayed a low total activity in the ^{3}H-assay. It was not tested in a ^{1}H-NMR experiment.

To investigate the roles of proposed catalytic acid and base in the reaction, we created the active site variants Y149A, Y149F, Y149H, H154F, and H154Y. All three variants at position 149 have a residual activity of around 0.5 % of wild type, as seen in Table 1. H154Y displays a similar level of residual lyase activity, whereas the activity of H154F was close to the detection limit. The other two proposed active site residues D152 and D178 were also investigated, creating variants D152E, D152N, D178E, D178N, and D178R. D152N and D178N both display a higher residual activity than D152E and D178E. This implies that the size of these residues is more important than their negative charge, and this is the opposite of what we observe for the other two aspartates D119 and D173. The D178R variant was inactive, which is not unexpected for such a

dramatic change in the active site. ^{1}H-NMR experiments were not performed for any of these variants.

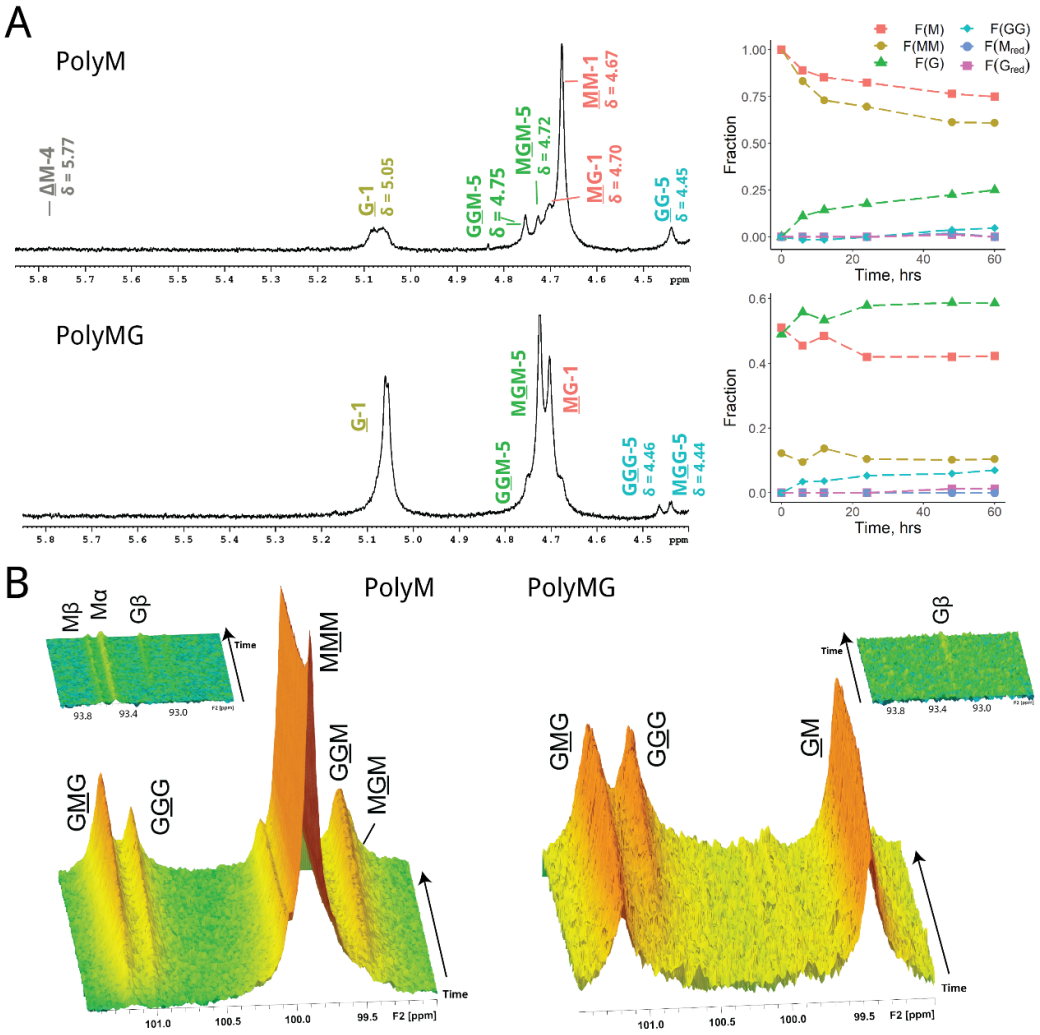

Figure 5: NMR-spectra showing R148G activity on polyM and polyMG. Underlined monomer residues give rise to the signals, and they give distinct peaks based on their nearest neighbour residues. A: ^{1}H spectra after epimerization for 60 h, in 5 mM HEPES, 75 mM NaCl, 2.5 mM $CaCl_2$, pH 7.0. 2.5 mg/ml of substrate and 0.092 µM of enzyme were added (1:300 enzyme:substrate, w/w). Plots show fractions calculated from integration of spectra recorded at different time points of the reactions. B: Time resolved ^{13}C-spectra from 0-1000 min (16.7 h), recorded at 25 °C with 10 mM MOPS, 75 mM NaCl, 2.5 mM $CaCl_2$ and pH 7.0. 11 mg/ml of substrate and 3.0 µM of enzyme were used (1:42 enzyme:substrate, w/w).

Complex effects on the dual activities are observed by varying reaction conditions

It is already known that the lyase activity of AlgE7 decreases with increasing NaCl concentrations, and at 300 mM the activity is reduced to one tenth of the wild type (23). Epimerization activity for the AlgEs, on the other hand, has been found to be promoted by or at least insensitive to intermediate concentrations of NaCl (100-200 mM) (31, 32). As already mentioned, we observed a change in the product profile relative to previous studies, from a higher amount of reducing end M-residues to a higher amount of reducing end G-residues. We hypothesized that this was

due to our buffer for the time resolved reaction, which contained 75 mM NaCl to circumvent gel formation after epimerization. The addition of NaCl boosted the G-block production of both wild type and R148G, especially on polyMG (Table S1). The effect of NaCl was therefore investigated in more detail, to see if the relative activities were influenced by adding different NaCl concentrations. Other reaction conditions, varying the level of calcium, pH, and substrate concentration were also tested.

AlgE7 was subjected to a factorial experiment where combinations of added NaCl (0, 50, 150 and 300 mM), calcium chloride (0, 1 and 3 mM), pH (6, 7 and 8) and substrate (1 and 0.125 mg/ml) were tested. All the experiments contain from 0.16-0.25 mM calcium, stemming from the enzyme buffer, as calcium is required for the structural stability of the enzymes. Lyase activity was measured with a spectrophotometric assay detecting increase in A230 (shown in Figure S7), and the initial slope (Figure 6) and the end point values (Figure S8) were calculated. All values are listed in Table S3. The initial lyase activity of AlgE7 decreased with increasing NaCl concentrations, but the effect was lower when calcium was added. For 3 mM calcium, the activity at 50 mM NaCl was comparable to the activity at 0 mM NaCl without supplemented calcium. The optimal pH is 7 (also seen in (23)), and the activities at pH 6 and 8 were lower when comparing them at the same conditions. When no NaCl was present, the activity at pH 8 was around 1.5 times higher than at pH 6, but the activity at pH 6 was less affected by NaCl concentrations than at pH 8. Positively charged residues are involved in the substrate interaction, as well as in the lyase reaction through R148 and K172, and pH could affect protonation of these residues. Similar to what was observed previously (23), at high calcium concentrations and high substrate concentrations, 300 mM salt was not completely inhibiting the reaction except for at pH 8. All activities were naturally higher at the same reaction conditions when 1 mg/ml substrate was present than when 0.125 mg/ml was present, but the same trends are observed at the low and the high substrate concentration. An exception is at pH 6, no NaCl and 1-3 mM $CaCl_2$, where the enzyme has comparable activity on 0.125 mg/ml substrate as on 1 mg/ml. The enzyme kinetics cannot be modelled by classical Michaelis-Menten kinetics, due to the continuously changing substrate from cleavage and epimerization.

To analyse the epimerization and lyase reaction simultaneously, different NaCl and calcium concentrations at pH 7 with 9 mg/ml of polyM were tested with time-resolved NMR (Figure 6, bottom). The NMR-experiment is performed at higher substrate concentrations than the lyase assay in order to obtain a sufficient signal to noise ratio for NMR. From the integrated time points, we observed that at 0 mM added calcium, both the lyase and epimerase reactions proceeded more slowly than when calcium was added to the reaction buffer. In the experiments where the NaCl concentrations were changed, the calcium concentration was kept constant at 2.5 mM. The loss in G-block formation at 75 mM NaCl and 3 mM calcium, compared to at 1 mM calcium, emphasizes an inhibition of calcium on G-block formation. At high calcium concentrations (2.5 and 3 mM) and NaCl concentrations below 150 mM, almost no MGG-triads were produced, unlike at higher NaCl or lower calcium concentrations where MGG-signals were produced initially and then removed through cleavage. MG and GG formation were highest at 300 mM NaCl, but this was not explained by a decrease in lyase activity. The lowest lyase activity was seen at 150 mM NaCl, unlike in the lyase assay where the lowest activity was seen at 300 mM NaCl. An important difference between the lyase assay and the ^{1}H-NMR experiments is that in the latter, the substrate concentration is considerably higher (9 mg/ml, against 0.125-1 mg/ml in the lyase assay).

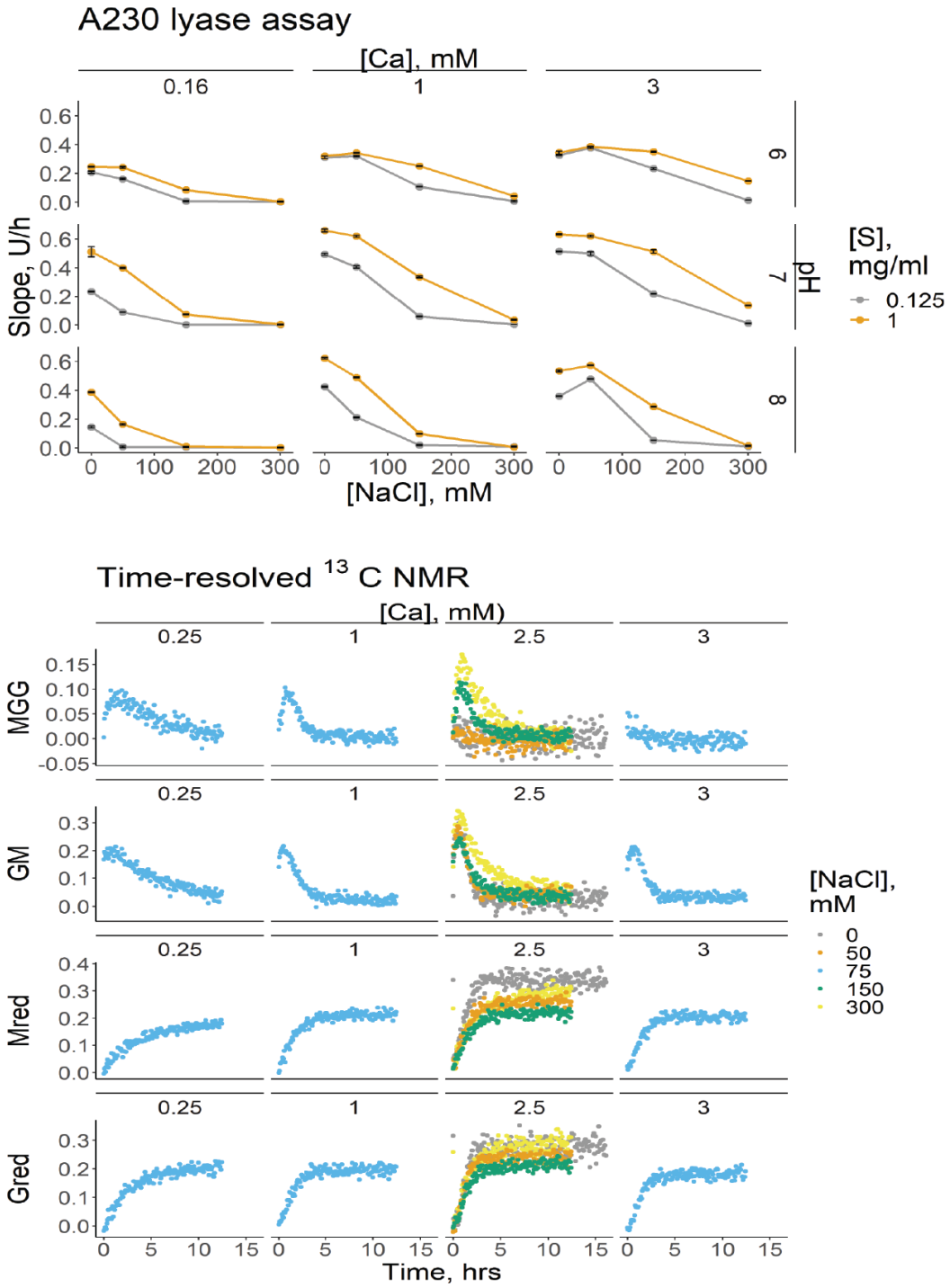

Figure 6: Salt dependency experiments of wild type AlgE7. Top: Slopes from a factorial spectrophotometric lyase activity assay at two different substrate concentrations [S], three different pHs, three different calcium concentrations, and four different NaCl concentrations. 0.3 µM of enzyme was added to each reaction. Slope is given in U/h, where U is absorbance units at 230 nm. Points are averages of two repetitions, and error bars show the range of values for the repetitions. Bottom: Integrated time points from ^{13}C NMR with constant [S] (9 mg/ml) and constant pH (6.9) at four different calcium and salt concentrations. 3 µM of enzyme was added to each reaction. Y-axes show the relative integrals of peaks representing the given residues.

Discussion

Mode of action of AlgE7 wild type

In the first experiments presented, we observed that the lyase and epimerase activities are affected by the substrate, which in turn results in different product pattern. When *A. vinelandii* secretes the alginate used in its protective coat, the alginate has already gone through modifications by periplasmic lyases and epimerases. AlgE7 and the other excreted epimerases and lyases therefore encounter a substrate that is not pure polyM. The activities of the extracellular enzymes partake in forming the final alginate product in complex ways, and this is clearly illustrated from the results we obtained using the bifunctional AlgE7 alone on different substrates.

Overall, AlgE7 has a much higher lyase activity when acting on polyM compared to polyMG, and it does not cleave pure G-substrate at all. From the NMR-results displayed in Figure 2, we find that when M-rich alginate is the substrate, the potential cleavage sites are G↓XM and M↓XM. When the substrate contains almost solely MG-alternating residues, G↓GM is the preferred cleavage site, as mainly G_{red} and ΔM are produced and the substrate contains almost no MM-sequences. Small peaks corresponding to ΔG and M_{red} also allows G↓XG, which is not found on polyM. The potential cleavage sites for both substrates are shown in Figure 7. As peaks for M<u>G</u>G and G<u>G</u>M are removed on polyM, and no consecutive G-residue signals are present in the HSQC-spectrum at the end of the reaction, the enzyme is likely able to create Δ-residues from G-residues also on polyM. It should be able to cleave M-residues, as we observe lyase activity from the start on polyM. AlgE7 does not appear able to create more than two consecutive G-residues on polyM before they are removed through cleavage events.

We hypothesize that both epimerization and cleavage could happen in the same binding event, where cleavage of the alginate chain represent the last step of the processive action before product dissociation and release. Alternatively, it could be the result of preferred attack at the reducing end of MG-blocks flanking M-blocks and G-blocks flanking MG-blocks. Both hypotheses could explain why we see approximately equal amounts of G- and M-residues at the reducing end of products created from polyM. It could also explain why we do not observe <u>Δ</u>G-signals on M-rich substrates, because if AlgE7 moves in the same direction as AlgE4 (21) it would only create those signals in the unlikely event that it reaches the end of another MG-block. It is supported by a larger <u>Δ</u>M-peak than Δ<u>M</u>G-peak from polyM (Figure 2B), because on an M-rich alginate, attacking the reducing end of G- and MG-blocks would be likely to produce ΔMM When the substrate is polyMG, half of the initial substrate is G-residues, and some <u>Δ</u>G signals are expected. According to the presented hypothesis we would also expect mainly G-reducing ends and almost no M-reducing ends, because cleavage would happen after the formation of G-blocks. The fact that the enzyme cannot cleave pure G-alginate also fits into this hypothesis, as this alginate cannot be epimerized. This is also seen from the chromatograms (Figure S5), where AlgE7 is found to create products that elute at approximately the same time as trimers, tetramers and pentamers created by lyase activity on polyM and polyMG, and not with products created by a G-lyase on polyG.

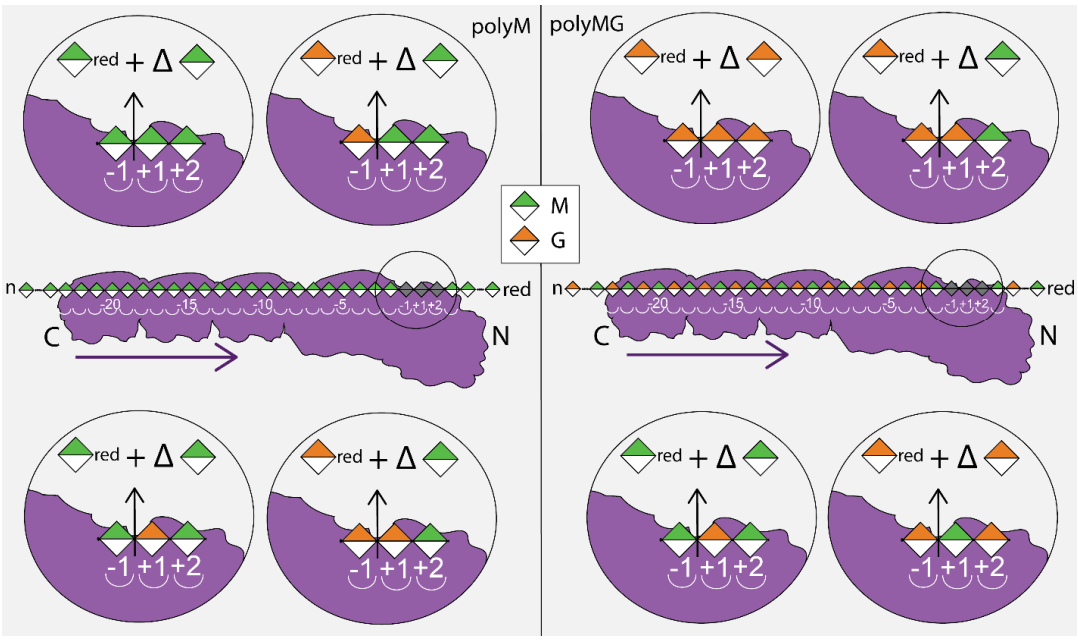

Figure 7: Illustration of the possible cleavage sites from the observed product patterns of AlgE7 on polyM (left) and polyMG (right). In the middle figures, AlgE7 is shown as it binds to the substrate it is presented with initially, but this will change during the reaction course. Except for M↓MM, all cleavage sites are in accordance with cleavage after a processive binding event, or due to preferred attack of the end of MG- and GG-sequences. For polyM, we observed creation of M_{red}, G_{red} and ΔM, which can be caused by cleavage at the four cleavage sites illustrated in the left figures. On polyMG, mainly G_{red} and ΔM are observed, corresponding to cleavage site G↓GM. However, we also observe small amounts of M_{red} and ΔG, and four cleavage sites shown in the right figures are possible on polyMG. Sugar residues are coloured according to the Symbol Nomenclature for Graphical Representations of Glycans (33). The purple arrows indicate the proposed direction of movement for the processive AlgE4 (21). AlgE7 consists of one A-module and three R-modules, and the outline of all four modules is shown. The spatial arrangement of these modules is suggested in the figure to be elongated, but this is not studied experimentally.

Features of the different potential substrates for the lyase reaction are probably important for the substrate specificity and product formation of the enzyme. Consecutive M-residues are more outstretched in the chain than alternating MG or consecutive G-residues. Two M-residues are around 10.5 Å long, whereas two consecutive G-residues are around 8.7 Å (34). In addition, M has a hydrophilic and a hydrophobic face, whereas G does not have a hydrophobic face. Our results support the previous findings that the epimerization pattern is important for the subsequent lyase product profile (23). When we study the two activities of AlgE7, it is important to keep this interaction in mind. Not only is the lyase activity affected by the epimerization, but the degradation of epimerized residues also hinders the measurement of the actual epimerization activity of the enzyme rendering this a challenging system for experimental investigation.

The enzymatic mechanism of epimerization and cleavage

The exact positioning of various substrates might determine if epimerization or cleavage happens, but the reason why only some of the AlgE epimerases like AlgE7 are bifunctional must be due to specific sequence determinants of the enzymes. Other AlgE epimerases like AlgE2 and AlgE5 perform only occasional cleavage events that could be the results of failed epimerizations (35, 36). We cannot know for sure which of the residues Y149 or H154 that is responsible for abstracting the proton (AA2 in Figure 1), but we propose that H154 is the proton abstractor and Y149 is the catalytic acid on M-residues (Figure 8). The directionality imposed by the observed products and displayed in Figure 7 seemingly rules out that Y149 could abstract the H-5 protons from M residues. This orientation is consistent with the one observed for a trimannuronate ligand

in the crystal structure of AlgE4, as well as previous docking experiments. The dual activity is thus likely governed by the exact positioning of Y149 relative to the substrate, and its closeness to either the C5 or the O4 of the residue in the +1 subsite. This is strongly supported by the sequence differences between ConL and ConE being largest around Y149, i.e. residues in positions 117, 148 and 172, as well as the activities of the mutants AvAlgE7-R148G, AvAlgE7-R148K, and AvAlgE7-E117K-K172L. We cannot be sure if the same residue performs proton abstraction of both M-residues and G-residues, as a G would be positioned differently in the active site. Alginate lyases that can cleave G-residues can perform an *anti* β-elimination using either a histidine or a tyrosine as a base, and a tyrosine as an acid (37, 38). Based on this, it cannot be ruled out that Y149 might perform the role of the base when the enzyme removes G-residues, as it might be in a better position for this than the histidine (seen in the last step of epimerization in Figure 8).The two active site aspartates D152 and D178 have been proposed to be associated with substrate stabilization in AlgE4 (19), and D178 could also neutralize the charge of the carboxylate group through the coordination of a calcium ion (24). For simplicity we have not shown the neutralization of the carboxylate charge in Figure 8.

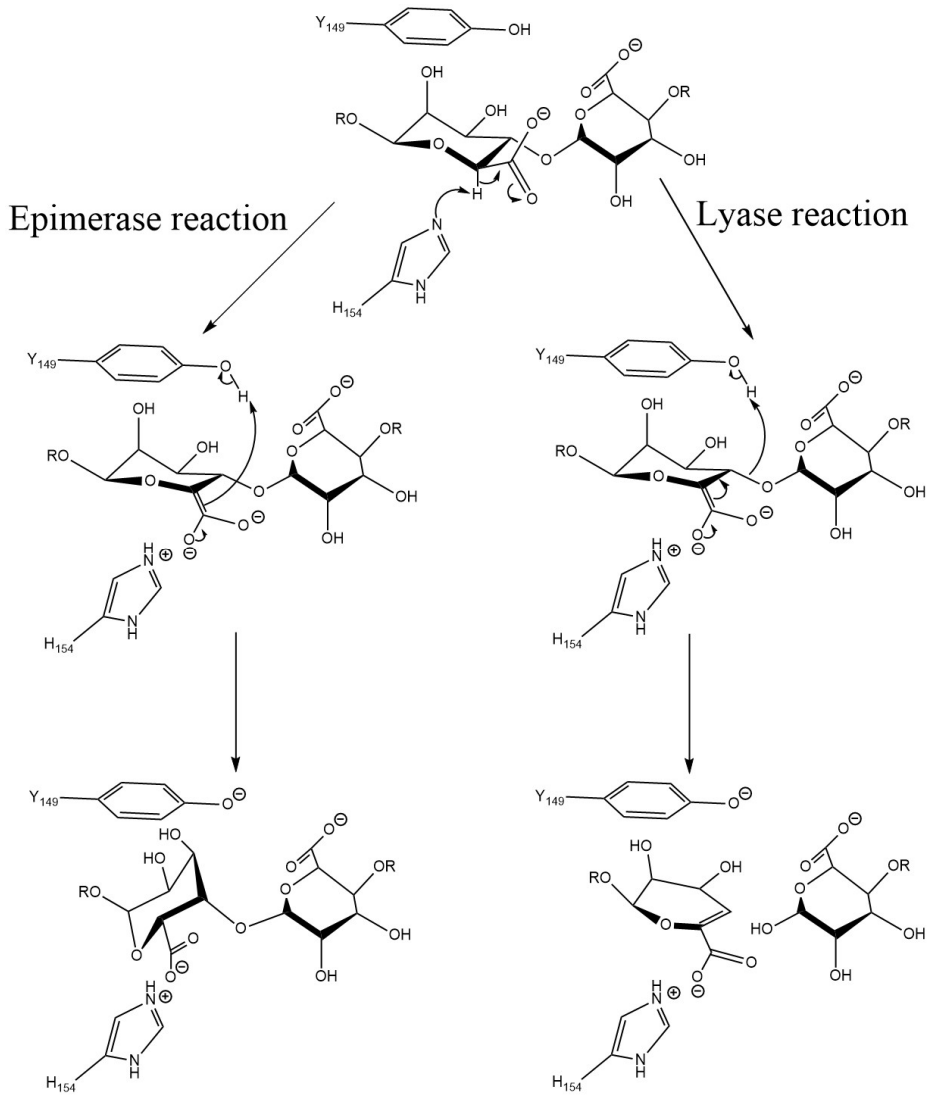

Figure 8: Proposed mechanisms of epimerization and lyase reaction of AlgE7 on M-residues (XMMX substrates).

E117, R148 and K172 might position the substrate residue in the active site and the active tyrosine Y149 through electrostatic interactions, as well as perturbing the pK_a of Y149 and of the substrate. This could influence whether Y149 donates the proton to the other face of the sugar ring (epimerization), or to the glycosidic bond (lyase reaction). R148 was shown to be the most important residue for the lyase activity of AlgE7. Based on the result that the R148K variant retains slightly more lyase activity than the R148G variant, the charge of R148 seems to be essential, whereas the guanidino group of the arginine is required for optimal activity (Table 1 and Figure 4). We have considered the possibility that R148 donates the proton to the glycosidic bond itself, but it is placed to the left of Y149 in Figure 8, and is therefore presumably too far from the glycosidic bond in the proposed reaction mechanism. Even in the enzyme where E117K, Y122F, R148G, and K172L substitutions are combined, a very weak lyase activity can be observed in the NMR-spectra (Figure 4). This supports the hypothesis that these residues set up the lyase reaction, but that they are not the ones performing it. Our results point to an amino acid being responsible for the lyase reaction, not a water molecule as has been previously proposed, as variants containing R148G lose almost all lyase activity.

The effects of the variants E117K, Y122F and K172L on the lyase activity was not as large as for R148. They did, however, produce more G-residues than M-residues at reducing ends, unlike the wild type that produce similar amounts. This was even more pronounced in the variant combining all three amino acid replacements. If we base the discussion on the scenario laid out in Figure 7, the cleavage event in the wild type acting on polyM happens randomly either at G|MM or M|XM. When this is changed in E117K, Y122F and K172L, it might be due to a change in the positioning of the substrate in the active site so that cleavage is more likely for G|MM than for M|XM. As mentioned, M- and G-residues have different lengths in a chain, and different hydrophilic/hydrophobic characteristics. They also have different configurations of all the polar groups around the ring carbons, and due to their opposed chair conformations ($^4C_1$ for M and $^1C_4$ for G), they give different three-dimensional structures to an alginate chain. For all these reasons, M-blocks, MG-blocks and G-blocks will orient differently in the enzyme binding groove, and the enzyme requires a fine-tuning of interacting residues to position different substrates properly for catalysis. E117 and K172 are both situated a bit away from the putative substrate binding site, and they are more likely to affect substrate binding indirectly through affecting R148 and Y149. E117 might be important for the hydrogen bond formed between D119 and R148. The inactivity of the Y122A variant implies that the aromaticity or the size of this residue is important. Similar results were obtained for AlgE4, where the F122Y variant retained 65 % of the wild type activity whereas the F122V variant only retained 0.2 % (19). AlgG has a tyrosine positioned in the corresponding position, and although the alanine variant of this residue was not detrimental, it reduced the activity to 20 % of the wild type activity compared to 66 % for the phenylalanine variant (24). For AlgG, it was concluded that this residue has a role in coordinating the active site histidine. Based on the results presented here, we also propose that it has a role in substrate interactions, and that Y122 helps in the correct positioning of the substrate for lyase activity.

The hydrogen bonding network between the charged residues around the active site are presumably important for the processive mode of action of all the AlgE epimerases, and not only for the catalytic mechanism. D119A, D173 and R195 are conserved in the block-forming AlgE epimerases, but there is no equivalents to them in AlgG that introduces occasional single G-residues in the alginate chains. In AlgE4, K117 forms a hydrogen bond with D119, which in turn is positioned close to the substrate and hydrogen bond with the backbone of Y149 (21). D119A in AlgE4 is not as detrimental to activity as it is in AlgE7 (Figure 4, Table 1), whereas the removal of the charges of D173 and R195 reduces activity dramatically (19, 21). On the other hand, the D173E variant retained half the activity of the wild type, whereas R195K retained only 3 %. Block-

formation requires either a processive action with the ability to stay attached to the substrate for consecutive catalytic events, or at least a preferred attack with the ability to bind specifically to already epimerized alginate chains. In both cases it would be related to the substrate interaction, and this might be the property that is affected when D119, D173 and R195 are mutated.

High NaCl-concentrations were seen to inhibit the initial lyase activity in the A230 lyase assay but not in the time-resolved NMR-experiments (Figure 6), and this could also be explained by effects on the substrate interaction. Na^+ and Cl^- ions could shield residues essential in substrate interaction that are not necessarily placed in the active site, and the charges on the substrate itself. In the time-resolved NMR-experiments substrate concentrations are higher (9 mg/ml, against 0.125-1 mg/ml in the lyase assay), when large amounts of substrate is present, the requirement for a strong enzyme-substrate interaction would be lowered as the enzyme could easily bind again after dissociation. Charged residues (E117, R148 and K172) are also implicated in the lyase reaction, but if shielding of these were detrimental, we would not expect that a high substrate concentration would diminish the effect. The loss in G-block formation at high calcium concentrations, but only when salt concentrations were low, probably stem from sodium ions shielding the charges in the MG-substrate, preventing it from forming junction zones with calcium that would render it inaccessible to subsequent G-block formation. We see that NaCl promotes formation of G-blocks for both wild type and R148G (Figure 2, Figure 5, Figure S4), and in the lyase-inactive variant this must be caused by an increase in epimerization activity, and not from a change in lyase specificity. At the low substrate concentrations in the lyase assay, this effect would be smaller, and here calcium is instead seen to save the activity at high NaCl concentration. It would be interesting to further investigate the effects from different substrate concentrations in the future, and this could be combined with an investigation of residue or module determinants of the substrate interaction and processive mode of action.

Conclusions

In summary, the results presented support previous data suggesting that the epimerisation and lyase activities in the bifunctional AlgE7 share the same catalytic site. The two activities affect each other, and the product formation is highly dependent on which substrate the enzyme is acting on. The lyase preferential cleavage sites are found to be M|XM and G|XM by using the well-defined alginate substrates polyM and polyMG. The mechanistic insights obtained through amino acid replacements and structural analysis suggest a more likely catalytic reaction mechanism on M-residues, where H154 acts as a catalytic base (or AA2) in the reaction, and Y149 takes the role as a catalytic acid (or AA3). The variant R148G, positioned next to the catalytic residue Y149, abolished almost all lyase activity but retained epimerisation activity. For the lyase reaction, R148 may affect whether Y149 donates the proton to the glycosidic bond or to the other side of the sugar ring. Cleavage of G-residues is also evident from the identified reaction products. The reaction conditions affect the enzymatic activity, where higher NaCl reduces the lyase active and increase G-block formation, whereas high calcium concentrations increase lyase activity and decrease G-block formation. The findings in this study explain the mechanistic basis behind the dual activity of AlgE7, in comparison to the AlgEs with mainly epimerase activity. New insight into how the two activities can be modulated relative to each other, both in terms of amino acid residues and reaction conditions, will aid in future applications of the AlgEs on tailoring of alginates.

Experimental procedures

Alginate substrates

All alginate substrates were freeze dried and weighed out upon use. Polymannuronan (polyM) was produced from the epimerase deficient AlgG *Pseudomonas fluorescens* strain PF20118 (NCIMB 10525) (39). This substrate has an F(MM) of 1.00, and a DP_n of around 370 determined from its molecular weight averages with Size-exclusion chromatography with multi-angle light scattering (SEC-MALS) (M_n of 73 kDa and M_w of 146 kDa) (Aarstad et al. 2019). ^{13}C-1 labelled polyM was produced from fermentation of the same strain, but using ^{13}C-1 (99 % ^{13}C) D-fructose (Cambridge Isotope Laboratories, USA). This substrate was further subjected to acid hydrolysis as described elsewhere (40, 41), and had a final DPn of around 70. [5-^{3}H]-labelled mannuronan was produced by growing the same strain on [5-^{3}H]-labelled glucose (Amersham). PolyMG was produced by epimerizing pure polyM with AlgE4 epimerase (42), until reaction completion, obtaining a final F(G) of 0.46 and F(GG) of 0. ^{13}C-labeled polyMG was created in the same way, using ^{13}C-polyM. This substrate was subjected to acid hydrolysis, obtaining a DP_n of around 80. ^{13}C-labelled OligoG was produced by *in vitro* epimerization of ^{13}C-labeled polyM with AlgE1 epimerase, and then subjecting this product to acid hydrolysis (4, 43) to obtain a final DP_n of around 21 and an F(G) of 0.97.

3.2 Mutagenesis, protein production and purification

Table 2 Plasmids used in this study. Sequences can be provided upon request.

Plasmids	Description	Reference
pTYB1	Expression vector	New England Biolabs
pBG27	pTRc99a derivative, contains *AlgE7* gene	(11)
pKK2	pBG27 with *AlgE7*-E117L	This study
pRS16	pBG27 with *AlgE7*-E117K	This study
pRS38	pBG27 with *AlgE7*-D119A	This study
pRS39	pBG27 with *AlgE7*-D119E	This study
pRS40	pBG27 with *AlgE7*-D119N	This study
pKK3	pBG27 with *AlgE7*-Y122A	This study
pRS17	pBG27 with *AlgE7*-Y122F	This study
pTB95	pBG27 with *AlgE7*-R148G	This study
pJR4	pBG27 with *AlgE7*-R148K	This study
pJR3	pBG27 with *AlgE7*-Y149A	This study
pRS18	pBG27 with *AlgE7*-Y149F	This study
pRS35	pBG27 with *AlgE7*-Y149H	This study
pRS19	pBG27 with *AlgE7*-D152E	This study
pRS20	pBG27 with *AlgE7*-D152N	This study
pRS22	pBG27 with *AlgE7*-H154F	This study
pRS21	pBG27 with *AlgE7*-H154Y	This study
pJR1	pBG27 with *AlgE7*-K172L	This study
pJR2	pBG27 with *AlgE7*-K172R	This study
pKK5	pBG27 with *AlgE7*-D173A	This study
pRS23	pBG27 with *AlgE7*-D178E	This study
pRS24	pBG27 with *AlgE7*-D178N	This study
pRS25	pBG27 with *AlgE7*-D178R	This study
pRS26	pBG27 with *AlgE7*-R195L	This study
pKK7	pBG27 with *AlgE7*-H196A	This study

pKK10	pBG27 with *AlgE7*-E117K-R148G	This study
pKK11	pBG27 with AlgE7-E117K-R148G-K172L	This study
pJR5	pBG27 with *AlgE7*-R148K-K172L	This study
pJR6	pBG27 with *AlgE7*-R148K-K172R	This study
pTB113	pBG27 with *AlgE7*-E117K-Y122F-R148G	This study
pTB118	pBG27 with *AlgE7*-E117K-Y122F-K172L	This study
pTB119	pBG27 with *AlgE7*-E117K-Y122F-K172R	This study
pTB111	pBG27 with *AlgE7*-E117K-Y122F-R148G-K172L	This study
pTB112	pBG27 with *AlgE7*-E117K-Y122F-R148G-K172R	This study
pTB116	pBG27 with *AlgE7*-E117K-Y122F-Y149A	This study

Plasmids encoding AlgE7 variants (Table 2) were constructed based on wild type AlgE7 (plasmid pBG27) (11) using the QuikChange™ Site-directed Mutagenesis Kit (Stratagene/Agilent) or Q5 site directed mutagenesis (New England Biolabs), according to instructions by the manufacturers. Primer sequences can be provided upon request. All cloning was done in *E. coli* DH5α competent cells (New England Biolabs).

Extracts of the variants and wild type used in the A230 lyase activity assay were produced in 96 well plates as previously described (20). AlgE7 variant proteins and the wild type AlgE7 were expressed and purified in two different ways. Enzymes were partially purified after expression in DH5α *E. coli* competent cells at 37 °C, by fast protein liquid chromatography on a HiTrap-Q column (GE Healthcare), using two purification buffers and a disruption buffer containing 20 mM MOPS (pH 6.9) supplemented with 2 mM $CaCl_2$, 2 mM $CaCl_2$, 1 M NaCl, and 4 mM $CaCl_2$, respectively. AlgE7 and R148G were purified completely, by expressing the proteins in the pTYB1 vector containing a C-terminal intein tag in T7 Express competent *E. coli* cells (New England Biolabs) and purifying enzyme extract with affinity chromatography through the IMPACT™-CN system (New England Biolabs). Elution was done in HEPES buffer (20 mM HEPES, 5 mM $CaCl_2$, 500 mM NaCl, pH 6.9) and dialysed in 5 mM HEPES and 5 mM $CaCl_2$ to remove DTT and NaCl from the purification buffer, before they were freeze dried for storing.

Protein concentrations were estimated by the Bio-Rad protein assay (Bio-Rad) (44), or from the absorbance at 280 nm using a NanoDrop spectrophotometer, and extinction coefficients were calculated with the ExPASy ProtParam online tool (45).

Activity assays

Two assays were performed for the AlgE7 variants, the tritium assay and the A230 assay. Tritium assay was performed on partially purified enzymes by measuring the liberation of ^3H from [5-^3H]-mannuronan, essentially as described previously (29). The alginate substrate and product is precipitated and removed from the sample before measuring the liberated ^3H. Incubation with excess enzyme or prolonged incubation with a lyase will prevent efficient precipitation of the substrate due to the resulting short alginate oligomers, leading to an overestimation of the activity. Thus, appropriate enzyme amounts and incubation times were identified to optimize this assay. Reaction buffer contained 20 mM MOPS (pH 6.9), and 2mM $CaCl_2$, and reactions were incubated at 37 °C. The A230 absorbance assay was performed for crude enzyme extracts of variants by adding 20 µL of extracts to total reactions of 250 µL, 1 mg/ml polyM, in 50 mM Tris-buffer with 2.5 mM $CaCl_2$. Absorbance was measured in COSTAR UV microplates every five minutes for 18 hours at 25 °C, in a Spectramax ABS Plus microplate reader.

For AlgE7 purified with the IMPACT™-CN protocol, the A230 assay was performed in 50 mM Tris-buffer with various concentrations of NaCl (0, 50, 150, and 300 mM), $CaCl_2$ (0, 1, and 3 mM), pH (6, 7, and 8), and polyM substrate (0.125 and 1 mg/ml), with a constant enzyme concentration of 0.3 µM. The reactions were performed in COSTAR UV 96 well plates, measuring absorbance at 230 nm every third minute, for 7-18 hours (until an end point was reached) at 25 °C. All reaction mixes contained 0.16 mM $CaCl_2$ originating from the enzyme buffer. Each combination was performed twice.

Product patterns with NMR and HPAEC-PAD

0,25 % w/v (2.5 mg/ml) of polyM or polyMG were dissolved in 5 mM HEPES buffer and 2.5 mM $CaCl_2$, pH 6.9. AlgE7 and R148G purified with the IMPACT-CN protocol were added to a 1:300 w/w ratio with substrate, to final concentrations of about 8.3 µg/ml. The reactions were left at 25 °C for different time intervals. Reactions were stopped by adding EDTA to a final concentration of 5 mM, heated at 90 °C for 15 minutes and subsequently freeze dried. The samples were then dissolved in 600 µL D_2O with 20 µL 0.3 M triethylenetetraamine-hexaacetate (TTHA), pH 7, as a calcium chelator, and 2.5 µL 1% 3-(trimethylsilyl)-propionic-2,2,3,3-d_4 acid sodium salt (TSP) as a reference. NMR acquisition was done on a BRUKER AVIIIHD 400 MHz equipped with 5 mm SmartProbe (Bruker Biospin AG, Fällenden, Switzerland) at the NV-NMR-Centre/Norwegian NMR Platform (NNP) at the Norwegian University of Science and Technology (NTNU), a 30 ° flip angle pulse, 64 scans and a spectral width of 10 ppm. All spectra were recorded at 90 °C to decrease sample viscosity for increased resolution, and to move the solvent peak away from the chemical shift region of alginate. Integrations of spectra were done in TopSpin, and peaks were assigned as described previously (11, 46, 47). Sequential parameters were calculated according to the procedure in Supporting Information.

High-performance anion-exchange chromatography with pulsed amperometric detection (HPAEC-PAD) was performed for the last time points of the AlgE7 reaction on polyM and polyMG (60 h), using oligomeric standards created by degradation of polyM and polyMG by an M-lyase from *Haliotis tuberculata*, and degradation of polyG by the G-lyase AlyA from *Klebsiella pneumonia* as previously described (43, 48).

Time-resolved NMR

Time resolved ^{13}C NMR experiments following the epimerization reaction were performed as previously described (13, 21), using 10 mg/ml of $^{13}C1$ enriched polyM, oligoG and polyMG. AlgE7 and R148G purified with the IMPACT-CN protocol were added to final concentrations of 2.8-2.9 µM. The buffer contained 10 mM MOPS pH 6.9, 75 mM NaCl, and 2.5 mM $CaCl_2$, in 99.8% D_2O. For the wild type, the same experiment was also performed with varying concentrations of NaCl (0, 50, 75, 150, and 300 mM) and calcium (0, 1, 2.5, and 3 mM). After completion of the time-resolved experiment, a ^{13}C-^{1}H Heteronuclear Single Quantum Coherence (HSQC) spectrum was recorded for assignment of the products formed during the enzymatic reaction. The time resolved data was acquired on 25 °C using a Bruker Avance III HD 800 MHz spectrometer (Bruker Biospin AG, Fällenden, Switzerland) equipped with a 5-mm Z-gradient CP-TCI (H/C/N) cryogenic probe at the NV-NMR-Centre/NNP at NTNU. All NMR spectra were recorded using TopSpin version 3.5.7. and processed in TopSpin version 4.0.8. software (Bruker BioSpin).

Data availability

All data is contained within this manuscript and the Supporting Information.

Supporting information

This article contains supporting information. The Supporting Information section sites the following references: (43, 47).

Acknowledgements

We thank Rannveig Skrede for constructing the pRSxx plasmids, Karoline Kongsrud for constructing the pKKx plasmids, Jan Riedl for constructing the pJRx plasmids, Randi Aune for performing lyase activity assays, Olav Aarstad for performing the HPAEC-PAD analysis, and Wenche Iren Strand for assisting in NMR-analyses of lyase products.

Funding and additional information

This research was funded by the Research Council of Norway through grants 294946 (The Norwegian Seaweed Biorefinery Platform), 250875 (Alginate Epimerase), and 226244 (Norwegian NMR platform- NNP).

Conflict of interest

The authors declare that they have no conflicts of interest with the contents of this article.

References

1. Mørch, Ý. A., Donati, I., Strand, B. L., and Skjåk-Bræk, G. (2007) Molecular engineering as an approach to design new functional properties of alginate. *Biomacromolecules*. **8**, 2809–2814
2. Szekalska, M., Puciłowska, A., Szymańska, E., Ciosek, P., and Winnicka, K. (2016) Alginate: Current use and future perspectives in pharmaceutical and biomedical applications. *International Journal of Polymer Science*. **2016**, e7697031
3. Moradali, M. F., Ghods, S., and Rehm, B. H. A. (2018) Alginate Biosynthesis and Biotechnological Production. in *Alginates and Their Biomedical Applications* (Rehm, B. H. A., and Moradali, M. F. eds), pp. 1–25, Springer Series in Biomaterials Science and Engineering, Springer, Singapore, 10.1007/978-981-10-6910-9_1
4. Tøndervik, A., Aarstad, O. A., Aune, R., Maleki, S., Rye, P. D., Dessen, A., Skjåk-Bræk, G., and Sletta, H. (2020) Exploiting mannuronan C-5 epimerases in commercial alginate production. *Marine Drugs*. **18**, 565
5. Haug, A., Larsen, B., and Smidsrød, O. (1966) A study on the constitution of alginic acid by partial acid hydrolysis. *Acta Chemica Scandinavica*. **5**, 271–277
6. Haug, A., Larsen, B., Smidsrød, O., Eriksson, G., Blinc, R., Paušak, S., Ehrenberg, L., and Dumanović, J. (1967) Studies on the sequence of uronic acid residues in alginic acid. *Acta Chemica Scandinavica*. 10.3891/acta.chem.scand.21-0691
7. Draget, K. I., Skjåk Bræk, G., and Smidsrød, O. (1994) Alginic acid gels: the effect of alginate chemical composition and molecular weight. *Carbohydrate Polymers*. **25**, 31–38
8. Grant, G. T., Morris, E. R., Rees, D. A., Smith, P. J. C., and Thom, D. (1973) Biological interactions between polysaccharides and divalent cations: The egg-box model. *FEBS Letters*. **32**, 195–198
9. Gacesa, P. (1987) Alginate-modifying enzymes: A proposed unified mechanism of action for the lyases and epimerases. *FEBS Letters*. **212**, 199–202
10. Ertesvåg, H., Høidal, K. H., Hals, K. I., Rian, A., Doseth, B., and Valla, S. (1995) A family of modular type mannuronan C-5-epimerase genes controls alginate structure in *Azotobacter vinelandii*. *Molecular Microbiology*. **16**, 719–731
11. Svanem, B. I. G., Skjåk-Bræk, G., Ertesvåg, H., and Valla, S. (1999) Cloning and expression of three new *Azotobacter vinelandii* genes closely related to a previously described gene family encoding mannuronan C-5-epimerases. *Journal of Bacteriology*. **181**, 68–77
12. Bjerkan, T. M., Bender, C. L., Ertesvåg, H., Drabløs, F., Fakhr, M. K., Preston, L. A., Skjåk-Bræk, G., and Valla, S. (2004) The *Pseudomonas syringae* genome encodes a combined mannuronan C-5-

epimerase and O-acetylhydrolase, which strongly enhances the predicted gel-forming properties of alginates. *J. Biol. Chem.* **279**, 28920–28929

13. Gawin, A., Tietze, L., Aarstad, O. A., Aachmann, F. L., Brautaset, T., and Ertesvåg, H. (2020) Functional characterization of three *Azotobacter chroococcum* alginate-modifying enzymes related to the *Azotobacter vinelandii* AlgE mannuronan C-5-epimerase family. *Scientific Reports*. **10**, 12470
14. Lombard, V., Golaconda Ramulu, H., Drula, E., Coutinho, P. M., and Henrissat, B. (2014) The carbohydrate-active enzymes database (CAZy) in 2013. *Nucleic Acids Res*. **42**, D490–D495
15. cazy.org (2021) Carbohydrate-Active enZYmes Database
16. Hartmann, M., Holm, O. B., Johansen, G. A. B., Skjåk-Braek, G., and Stokke, B. T. (2002) Mode of action of recombinant *Azotobacter vinelandii* mannuronan C-5 epimerases AlgE2 and AlgE4. *Biopolymers*. **63**, 77–88
17. Campa, C., Holtan, S., Nilsen, N., Bjerkan, T. M., Stokke, B. T., and Skjåk-Bræk, G. (2004) Biochemical analysis of the processive mechanism for epimerization of alginate by mannuronan C-5 epimerase AlgE4. *Biochemical Journal*. **381**, 155–164
18. Bjerkan, T. M., Lillehov, B. E., Strand, W. I., Skjåk-Bræk, G., Valla, S., and Ertesvåg, H. (2004) Construction and analyses of hybrid *Azotobacter vinelandii* mannuronan C-5 epimerases with new epimerization pattern characteristics. *Biochemical Journal*. **381**, 813–821
19. Rozeboom, H. J., Bjerkan, T. M., Kalk, K. H., Ertesvåg, H., Holtan, S., Aachmann, F. L., Valla, S., and Dijkstra, B. W. (2008) Structural and mutational characterization of the catalytic A-module of the mannuronan C-5-epimerase AlgE4 from *Azotobacter vinelandii*. *The Journal of Biological Chemistry*. **283**, 23819–23828
20. Tøndervik, A., Klinkenberg, G., Aachmann, F. L., Svanem, B. I. G., Ertesvåg, H., Ellingsen, T. E., Valla, S., Skjåk-Bræk, G., and Sletta, H. (2013) Mannuronan C-5 epimerases suited for tailoring of specific alginate structures obtained by high-throughput screening of an epimerase mutant library. *Biomacromolecules*. **14**, 2657–2666
21. Gaardløs, M., Samsonov, S., Sletmoen, M., Hjørnevik, M., Sætrom, G. I., Tøndervik, A., and Aachmann, F. L. (2021) Insights into the roles of charged residues in substrate binding and mode of action of mannuronan C-5 epimerase AlgE4. *Glycobiology*
22. Stanisci, A., Tøndervik, A., Gaardløs, M., Lervik, A., Skjåk-Bræk, G., Sletta, H., and Aachmann, F. L. (2020) Identification of a pivotal residue for determining the block structure-forming properties of alginate C-5 epimerases. *ACS Omega*. 10.1021/acsomega.9b04490
23. Svanem, B. I. G., Strand, W. I., Ertesvåg, H., Skjåk-Bræk, G., Hartmann, M., Barbeyron, T., and Valla, S. (2001) The catalytic activities of the bifunctional *Azotobacter vinelandii* mannuronan C-5-epimerase and alginate lyase AlgE7 probably originate from the same active site in the enzyme. *The Journal of Biological Chemistry*. **276**, 31542–31550
24. Wolfram, F., Kitova, E. N., Robinson, H., Walvoort, M. T. C., Codée, J. D. C., Klassen, J. S., and Howell, P. L. (2014) Catalytic mechanism and mode of action of the periplasmic alginate epimerase AlgG. *The Journal of Biological Chemistry*. **289**, 6006–6019
25. Haug, A., and Larsen, B. (1971) Biosynthesis of alginate: Part II. Polymannuronic acid C-5-epimerase from *Azotobacter vinelandii* (Lipman). *Carbohydrate Research*. **17**, 297–308
26. Aachmann, F. L., Svanem, B. I. G., Güntert, P., Petersen, S. B., Valla, S., and Wimmer, R. (2006) NMR Structure of the R-module A parallel β-roll subunit from an *Azotobacter vinelandii* mannuronan C-5 epimerase. *J. Biol. Chem.* **281**, 7350–7356
27. Waterhouse, A., Bertoni, M., Bienert, S., Studer, G., Tauriello, G., Gumienny, R., Heer, F. T., de Beer, T. A. P., Rempfer, C., Bordoli, L., Lepore, R., and Schwede, T. (2018) SWISS-MODEL: homology modelling of protein structures and complexes. *Nucleic Acids Res*. **46**, W296–W303
28. Krieger, E., Joo, K., Lee, J., Lee, J., Raman, S., Thompson, J., Tyka, M., Baker, D., and Karplus, K. (2009) Improving physical realism, stereochemistry, and side-chain accuracy in homology modeling: Four approaches that performed well in CASP8. *Proteins*. **77 Suppl 9**, 114–122
29. Skjåk-Bræk, G., and Larsen, B. (1982) Biosynthesis of alginate part 5. A new assay for mannuronan C-5-epimerase activity. *Carbohydr. Res.* **103**, 133–136
30. Skjåk-Bræk, G., and Larsen, B. (1985) Biosynthesis of alginate: Purification and characterisation of mannuronan C-5-epimerase from *Azotobacter vinelandii*. *Carbohydrate Research*. **139**, 273–283
31. Ertesvåg, H., Høidal, H. K., Skjåk-Braek, G., and Valla, S. (1998) The *Azotobacter vinelandii* mannuronan C-5-epimerase AlgE1 consists of two separate catalytic domains. *The Journal of biological chemistry*. **273**, 30927–32

32. Høidal, H. K., Ertesvåg, H., Skjåk-Braek, G., Stokke, B. T., and Valla, S. (1999) The recombinant *Azotobacter vinelandii* mannuronan C-5-epimerase AlgE4 epimerizes alginate by a nonrandom attack mechanism. *The Journal of biological chemistry*. **274**, 12316–22
33. Varki, A., Cummings, R. D., Aebi, M., Packer, N. H., Seeberger, P. H., Esko, J. D., Stanley, P., Hart, G., Darvill, A., Kinoshita, T., Prestegard, J. J., Schnaar, R. L., Freeze, H. H., Marth, J. D., Bertozzi, C. R., Etzler, M. E., Frank, M., Vliegenthart, J. F., Lütteke, T., Perez, S., Bolton, E., Rudd, P., Paulson, J., Kanehisa, M., Toukach, P., Aoki-Kinoshita, K. F., Dell, A., Narimatsu, H., York, W., Taniguchi, N., and Kornfeld, S. (2015) Symbol Nomenclature for Graphical Representations of Glycans. *Glycobiology*. **25**, 1323–1324
34. Atkins, E. D. T., Mackie, W., and Smolko, E. E. (1970) Crystalline structures of alginic acids. *Nature*. **225**, 626–628
35. Ramstad, M. V., Ellingsen, T. E., Josefsen, K. D., Høidal, H. K., Valla, S., Skjåk-Bræk, G., and Levine, D. W. (1999) Properties and action pattern of the recombinant mannuronan C-5-epimerase AlgE2. *Enzyme and Microbial Technology*. **24**, 636–646
36. Holtan, S., Bruheim, P., and Skjåk-Bræk, G. (2006) Mode of action and subsite studies of the guluronan block-forming mannuronan C-5 epimerases AlgE1 and AlgE6. *Biochemical Journal*. **395**, 319–329
37. Ogura, K., Yamasaki, M., Mikami, B., Hashimoto, W., and Murata, K. (2008) Substrate recognition by family 7 alginate lyase from Sphingomonas sp. A1. *Journal of Molecular Biology*. **380**, 373–385
38. Garron, M.-L., and Cygler, M. (2010) Structural and mechanistic classification of uronic acid-containing polysaccharide lyases. *Glycobiology*. **20**, 1547–1573
39. Gimmestad, M., Sletta, H., Ertesvåg, H., Bakkevig, K., Jain, S., Suh, S., Skjåk-Bræk, G., Ellingsen, T. E., Ohman, D. E., and Valla, S. (2003) The *Pseudomonas fluorescens* AlgG protein, but not its mannuronan C-5-epimerase activity, is needed for alginate polymer formation. *Journal of Bacteriology*. **185**, 3515–3523
40. Abrahamson, M., Lewandowski, Z., Geesey, G., Skjåk-Bræk, G., Strand, W., and Christensen, B. E. (1996) Development of an artificial biofilm to study the effects of a single microcolony on mass transport. *Journal of Microbiological Methods*. **26**, 161–169
41. Ertesvåg, H., and Skjåk-Bræk, G. (1999) Modification of alginate using mannuronan C-5-epimerases. in *Carbohydrate Biotechnology Protocols* (Bucke, C. ed), pp. 71–78, Methods in Biotechnology™, Humana Press, Totowa, NJ, 10.1007/978-1-59259-261-6_6
42. Donati, I., Holtan, S., Mørch, Y. A., Borgogna, M., Dentini, M., and Skjåk-Bræk, G. (2005) New hypothesis on the role of alternating sequences in calcium−alginate gels. *Biomacromolecules*. **6**, 1031–1040
43. Aarstad, O. A., Tøndervik, A., Sletta, H., and Skjåk-Bræk, G. (2012) Alginate sequencing: An analysis of block distribution in alginates using specific alginate degrading enzymes. *Biomacromolecules*. **13**, 106–116
44. Bradford, M. M. (1976) A rapid and sensitive method for the quantitation of microgram quantities of protein utilizing the principle of protein-dye binding. *Analytical Biochemistry*. **72**, 248–254
45. Gasteiger, E., Hoogland, C., Gattiker, A., Duvaud, S., Wilkins, M. R., Appel, R. D., and Bairoch, A. (2005) Protein identification and analysis tools on the ExPASy server. in *The Proteomics Protocols Handbook*, pp. 571–607, Humana Press, Totowa, NJ, 10.1385/1-59259-890-0:571
46. Grasdalen, H. (1983) High-field, 1H-n.m.r. spectroscopy of alginate: sequential structure and linkage conformations. *Carbohydrate Research*. **118**, 255–260
47. Heyraud, A., Gey, C., Leonard, C., Rochas, C., Girond, S., and Kloareg, B. (1996) NMR spectroscopy analysis of oligoguluronates and oligomannuronates prepared by acid or enzymatic hydrolysis of homopolymeric blocks of alginic acid. Application to the determination of the substrate specificity of Haliotis tuberculata alginate lyase. *Carbohydrate Research*. **289**, 11–23
48. Ballance, S., Aarstad, O. A., Aachmann, F. L., Skjåk-Bræk, G., and Christensen, B. E. (2009) Preparation of high purity monodisperse oligosaccharides derived from mannuronan by size-exclusion chromatography followed by semi-preparative high-performance anion-exchange chromatography with pulsed amperometric detection. *Carbohydrate Research*. **344**, 255–259